



## INVESTIGATION OF HORST-GRABEN STRUCTURES AROUND GÜLŞEHİR (NEVŞEHİR-CENTRAL ANATOLIA) WITH PSINSAR AND LIDAR

Ramazan DEMİRCİOĞLU<sup>1\*</sup>, Osman OKTAR<sup>2</sup>

<sup>1</sup>Aksaray University, Department of Emergency Aid and Disaster Management, 68100, Aksaray, Türkiye


<sup>2</sup>Aksaray University, Department of Geomatics Engineering, 68100, Aksaray, Türkiye


**Abstract:** This study examined horst-graben structures in the study area using the Interferometric Synthetic Aperture Radar (PSInSAR) method, and the movements in the line of sight (LOS) were determined. Both field and PSInSAR and Lidar studies were evaluated together. Accordingly, the uplift observed in the horst-graben structures, and the descending movements observed in the grabens continue today. It has been observed that the faults forming the Horst and Graben structures are active. The structures determined by the field studies agree with the data obtained from the PSInSAR and Lidar studies. It has been determined that these structures continue to develop even today. The region continues to expand under the extensional tectonic regime.

**Keywords:** Türkiye, Central Anatolia, Horst-graben, GNSS, PSInSAR, Lidar

\*Corresponding author: Aksaray University, Department of Emergency Aid and Disaster Management, 68100, Aksaray, Türkiye

E mail: ra.demircioglu@gmail.com (R. DEMİRCİOĞLU)

Ramazan DEMİRCİOĞLU  <https://orcid.org/0000-0003-0616-0331>

Osman OKTAR  <https://orcid.org/0000-0001-6764-0561>

Received: May 08, 2024

Accepted: October 28, 2024

Published: March 15, 2024

**Cite as:** Demircioğlu M, Oktar O. 2024. Investigation of horst-graben structures around Gülşehir (Nevşehir-Central Anatolia) with PSInSAR and Lidar. BSJ Eng Sci, 8(2): xxx-xxx.

### 1. Introduction

The study area is located in the central Central Anatolian region (Figure 1). During the Neotectonic Era, specifically during the Late Miocene–Pliocene period. As a result of this transition, horst-graben formations and regular faulting were formed, extending in the NE-SW direction. The study area is northwest of the Ecemiş Fault Zone and east of the Tuzgölü Fault Zone, where both directional and normal faults are active. According to Koçyiğit (2003), Central Anatolia experienced an extensional tectonic regime oriented in the east-northeast and west-southwest directions during the neotectonic period. This conclusion is based on the geometry of morphotectonic structures and earthquake focal point solutions. In a separate study, Çiner et al. (2015) reported that basalt ages and cosmogenic data from the Kızılırmak River terraces in the Cappadocia Region indicated the valley was excavated by 160 meters over the last 2 million years. Additionally, they found that the regional uplift rate of the river in the Central Anatolian Plateau is approximately 0.08 mm per year, which has shown significant changes over time.

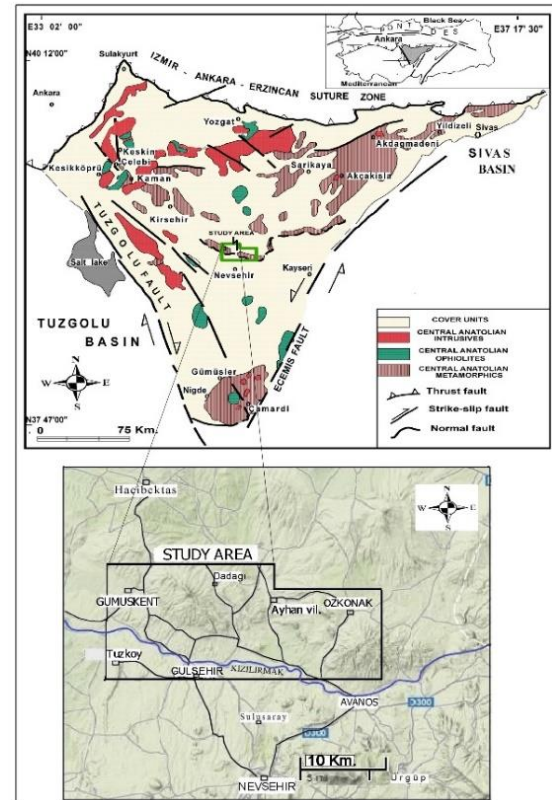


Figure 1. The study area.

The purpose of this study is to use the PSInSAR approach to determine the horst-graben structure and fault in the



studied area and reveal the motions of the region with the highest concentration of active faults. There are also studies on this subject. Some of them are (Biggs et al., 2007; Yavaşoğlu et al., 2011; Shirzaei, and Bürgmann, 2013; Zheng et al., 2013; Rosu et al., 2015; Wang and Jónsson, 2015; Gürsoy et al., 2017; He et al., 2018; Scott et al., 2020; Poyraz and Hastaoğlu, 2020; Wang et al., 2022; Eski and Sözbilir, 2024). The research area has been the subject of numerous studies, including works by (Aydın 1984; Atabey et al. 1988; Göncüoğlu et al. 1993; Temiz and Gökten, 2016; Koçak et al., 2021), sedimentological investigations by Atabey (1989), and structural geology studies by (Göncüoğlu et al., 1993; Dirik and Göncüoğlu 1996; Koçyiğit 2003; Doğan 2011). Finding the faults' surface deformations and tectonic movements that result in the local graben and horst structures is the aim of this investigation.

One unique aspect of this research is that there have been no previous geophysical and geodetic investigations on the horst-graben structures within the study region, which were identified through field investigations. Our findings indicate that detailed studies of geology and structural geology are supported by the velocity information derived from the analysis results.

## 2. Materials and Methods

Field studies were used to identify the Horst-Graben formations in the research zone, and PSInSAR was used to track the movement of the line of sight (LOS) in the area. In line with the findings of the Stanford Method for Persistent Scatterers (StaMPS)/MIT study (Hooper et al., 2018), PSInSAR analyses were performed on the examined region and compared to field study data.

To further illustrate the faults and morphology of the horst-graben structure in the research area, a cross-section was made. For a more thorough assessment of the fault morphology in the cross-section, Lidar data (from equatorstudios.com) were acquired, and a cross-section was generated using these data. This cross-section was produced using the Global Mapper program's data evaluation capabilities.

### 2.1. PSInSAR Analyses

To analyse crustal movement, Hooper et al. (2007) created the StaMPS software and used the PSInSAR technology, which was a novel approach. These techniques identify pixels with little phase change by employing spatial correlation of the interferometric phase. It can analyse any terrain in this way, even if structures or other things are present. Through the use of interferogram adaptation maps, fixed target sites are found. Establishing the correlation threshold value is the most basic evaluation technique.

The permanent scatterer (PS) point is designated for a target when it yields a fit value greater than the mean value. To increase the number of PS points, PSInSAR studies with at least 12 SAR images are advised (Hooper et al. 2018; Zhang et al., 2021; Zhou et al., 2022). Each image's pixel amplitude data are used to create the time

series. It is possible to identify highly suited targets by creating many sets of interferograms. For this purpose, a collection of differential interferograms is produced using a single master image. It is advised to utilise a DEM while creating interferograms to reduce the influence of topography.

### 2.2. PSInSAR Data Acquisition

Images from the European Space Agency's Sentinel-1 satellite were used in the PSInSAR analysis. The dates of the Sentinel-1A synthetic aperture radar (SAR) images are shown in Table 1, and the approximate coverage of the SAR (track 14) images is shown in Figure 2. In this study, 36 Sentinel-1 SAR images were used. The features of SAR images are interferometric wide (IW), C band, and track number 14, taken between January 2020 and December 2022.

SAR images were provided free of charge by the Copernicus Open Access Hub (URL-1).

**Table 1.** The Sentinel-1A synthetic aperture radar (SAR) images

2020.01.20	2021.01.14	2022.01.21
2020.02.13	2021.02.19	2022.02.26
2020.03.20	2021.03.15	2022.03.22
2020.04.13	2021.04.20	2022.04.15
2020.05.19	2021.05.14	2022.05.21
2020.06.24	2021.06.19	2022.06.14
2020.07.18	2021.07.13	2022.07.20
2020.08.23	2021.08.18	2022.08.23
2020.09.16	2021.09.23	2022.09.18
2020.10.22	2021.10.17	2022.10.24
2020.11.15	2021.11.22	2022.11.17
2020.12.21	2021.12.16	2022.12.11

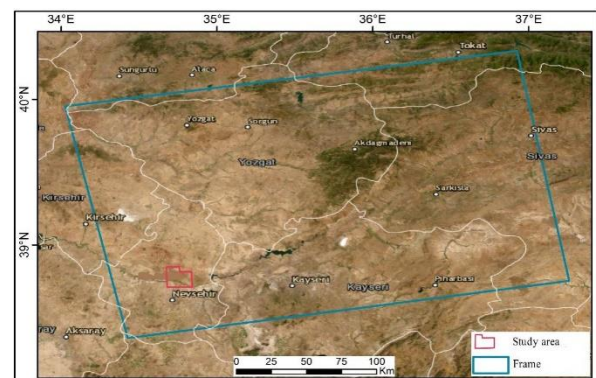


**Figure 2.** The blue box indicates the approximate coverage of the Sentinel-1A satellite radar images, track number 14.

## 3. Results

The research area's geological and geodetic investigations were assessed jointly. New information regarding the horst-graben structures in the area was discovered because of these investigations.

### 3.1. Study Area Geology and Structural Geology

The research region has rocks that are Paleozoic to Quaternary in age. The Kırşehir Massif's metamorphic units, which date from the Paleozoic to the Mesozoic era, make up the basement. Palaeocene-Quaternary aged units cover it in an unconformable manner (Figure 3). The studied region was originally impacted by compressional forces in roughly SW-NE directions, and subsequently in SE-NW directions throughout the Middle-Late Miocene period (Koçyiğit, 2003; Koçyiğit and Doğan, 2016; Demircioğlu, 2014).

In the Late Miocene-Pliocene period, the extensional tectonic regime is effective in the region, since there is no structure (reverse fault, fold, and inclined layers) to give any compressional tectonism in the units in the study area.

One of the signs that this extensional tectonic regime will continue is the cause of the activity on the Tuzgözü fault to the west of the study region and the Salanda fault within the study area. Additionally, there is a correlation between the significant fault strikes and the estimated principal stress orientations. The Kızılırmak valley in the study region is the greatest place to view the remnants of the extensional tectonic regime, which is believed to be continuing now. The data used in this study pertain to the extensional tectonic regime and are from the Pleistocene-Holocene, the younger units.

Local uplifts (Hırka horst) and basin formation continue with the extension. Although there are uplifts in Hırka Mountain and its surroundings (between Hırka Mountain and Ziyaret Hill), which are composed of Massif units, there are subsidences in the south of Hırka Horst, in the Kızılırmak valley (Kızılırmak Graben), and the north of Hırka Horst, around Kuyulukışla Village (Kuyulukışla Graben) (Figure 4).

Yüksekli, Dadağı, Salanda, Gülşehir, and Tuzköy faults are the main geological structures influencing the uplift and subsidence in the studied region. Based on these findings, the Neotectonic period is when the area acquired a horst-graben structure. Important neotectonic period structural components are the Kuyulukışla and Kızılırmak grabens, as well as the Hırka and Ziyarettepe horsts. The formation of the terrace systems in the valley is mostly due to the influence of climate conditions, specifically the Pleistocene Glacial period (Doğan, 2009).

In the research area, all fault types—normal, reverse, thrust, and strike-slip—can be observed. Every direction has faults, and the Massif contains every kind of rock. Poly-phase deformation is the cause of these faults. There is a lot of faulting within the cover units, particularly in the region known as the Ayhan fault zone. Because of the influence of the compressional tectonic regime, there is an impressive density of thrust and reverse faults in this region. These faultings are present in rocks of the Ayhan group that are from the Late Paleocene to the Middle Eocene. On the other hand, younger units have a lower fault density because they undergo less deformation. The Late Miocene (Messinian)–Pliocene dating units have

typically seen normal faulting because of the dominance of the extensional tectonic regime in the region (Figure 3).

The Hırka and Gezgintepe horsts were formed during this period by strike-slip faults with vertical displacement and normal faults (Salanda, Dadağı).

Grabens named Kuyulukışla and Kızılırmak formed in the space between these horsts. The region is still affected by the extensional tectonic regime. There were notable errors during this time. These important faults comprise the horst-graben structure.

The Salanda fault zone is a right-lateral strike-slip fault that also has a vertical displacement component. It is a strike-slip (transtensional) fault developing in an extensional tectonic regime.

There are visible portions of the Salanda fault (Figure 3, 4). There are two distinct fault strikes on the fault: N40-80°E and N45°W-N82°W. According to Demircioğlu and Oktar (2024), there are fault plane dips to the southwest and southeast with angles varying from 58 to 72 degrees (Demircioğlu, 2014). The vicinity of Eski Yaylacık hamlet is one of the research area's most visible locations (Figure 5). They stretch about between Gümüşkent Town and Eski yaylacık villages in the direction of N58°W. The fault in this region is roughly 10 kilometres long. Here, it creates the point where the basement units and the Yüksekli formation meet (Figure 3).

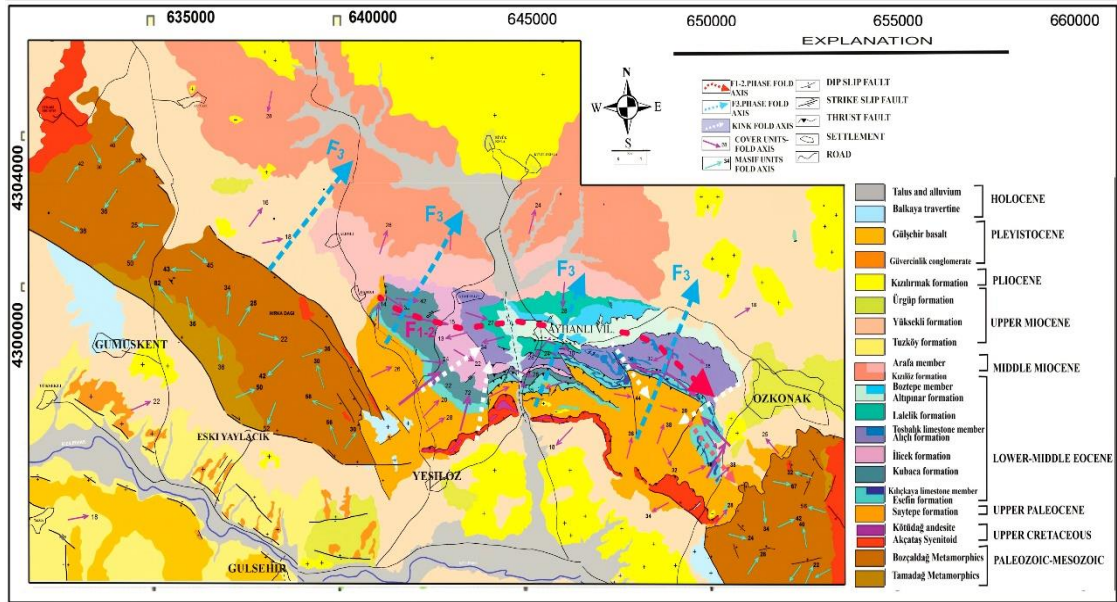


Figure 3. Geology-structural geological map of the study area (Modified from Demircioğlu, 2014).

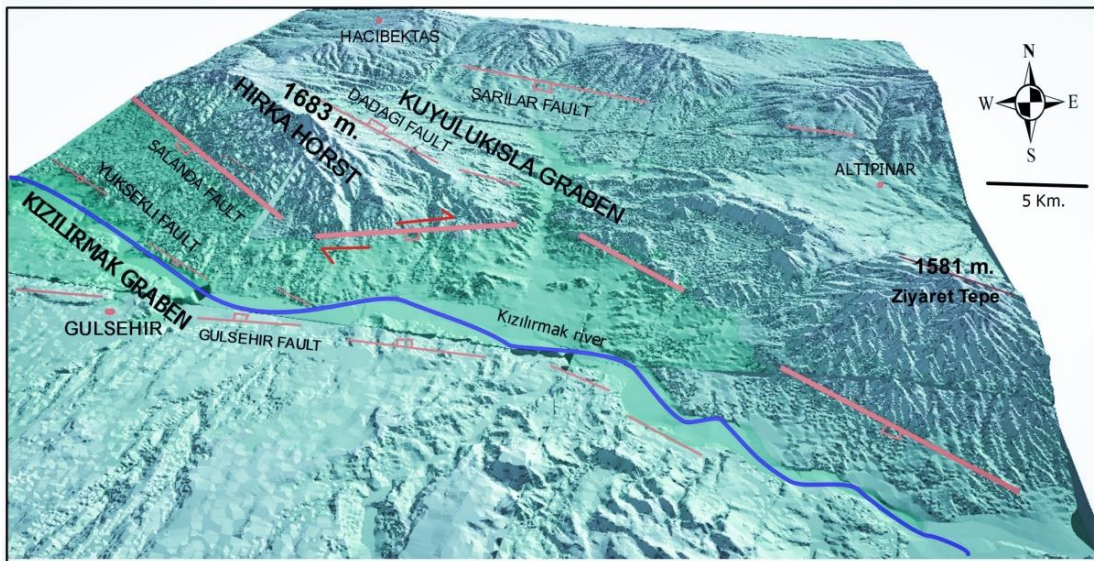
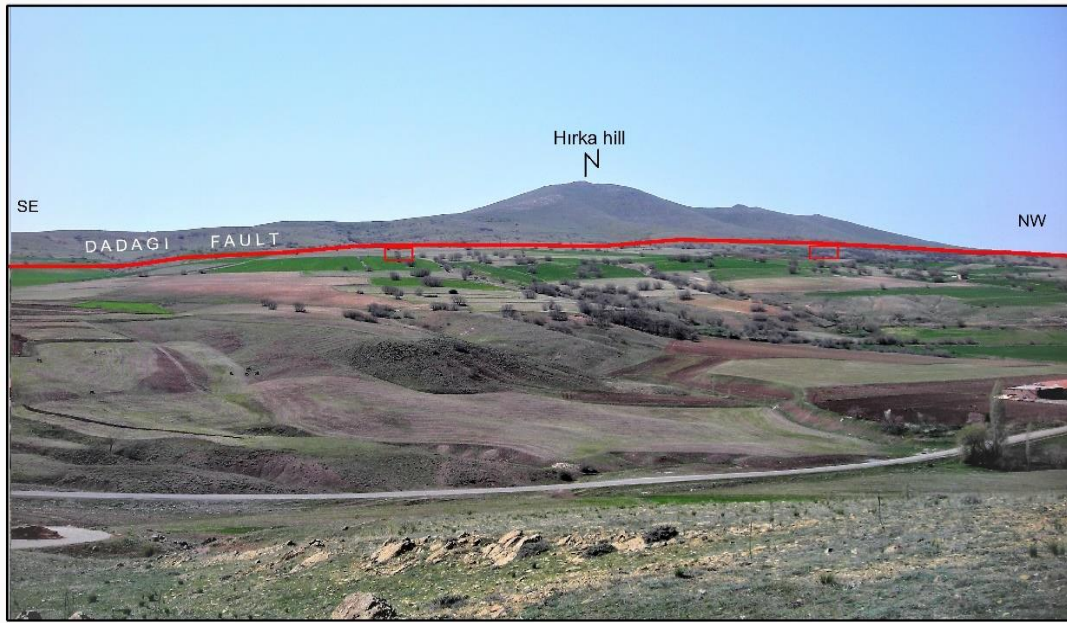


Figure 4. Morphotectonic view of the Salanda, Yüksekli, Gülşehir, Dadağı, and Sarılar faults (Modified from Demircioğlu, 2014).



Figure 5. View of the Salanda fault (Demircioğlu and Oktar, 2024).



**Figure 6.** General view of the Dadağı fault (Alemlı village).

Apart from the typical flaw, there's a lateral slip on the right side. They stretch between the villages of Yeşilöz and Eskiaylacık in the N58-720W direction. This section of the Salanda fault is roughly 7 kilometres long. They can be observed between Dondurma Hill and Yeşilöz Village in the northeast-southwest direction. Another way to think of this region is as a transfer fault. In this area, it is around 4 miles long. Present travertine developments are depending on this fault (Salanda) (Figure 5). This fault caused the formation of travertines, particularly in the northwest and northeast of Gümüşkent and in the area surrounding Balkaya Hill. Along the fault line, there are numerous water sources. The Dadağı fault is located in the portion of the massif that faces east (Figure 6).

They stretch between Höyük Tepe and Akçataş Village's

east in N60-680W directions (Figure 3, 4). The fault plane has a northeastern slope with dip angles that range from 52 to 65 degrees. It is about 15 km. long in this region. Around Höyük Tepe, at the southeast tip of the Dadağı fault, are travertine deposits.

The Salanda fault forms the boundary of the Massif's southwest region. In addition to this fault, they have led to the Massif rising and turning into a horst (Hırka horst). The Yüksekli fault (Figure 7) is one of the major faults of the Horst-graben complex. Along the route that connects Avanos District and Yüksekli Village, they outcrop fairly well. This fault and the Salanda fault are roughly aligned. It's a typical error. The Güvercinlik conglomerates are hung on a terrace-shaped, Pleistocene-aged Yüksekli fault. Compared to the Salanda fault, it is smaller. The Kızılırmak River is to the east of it.

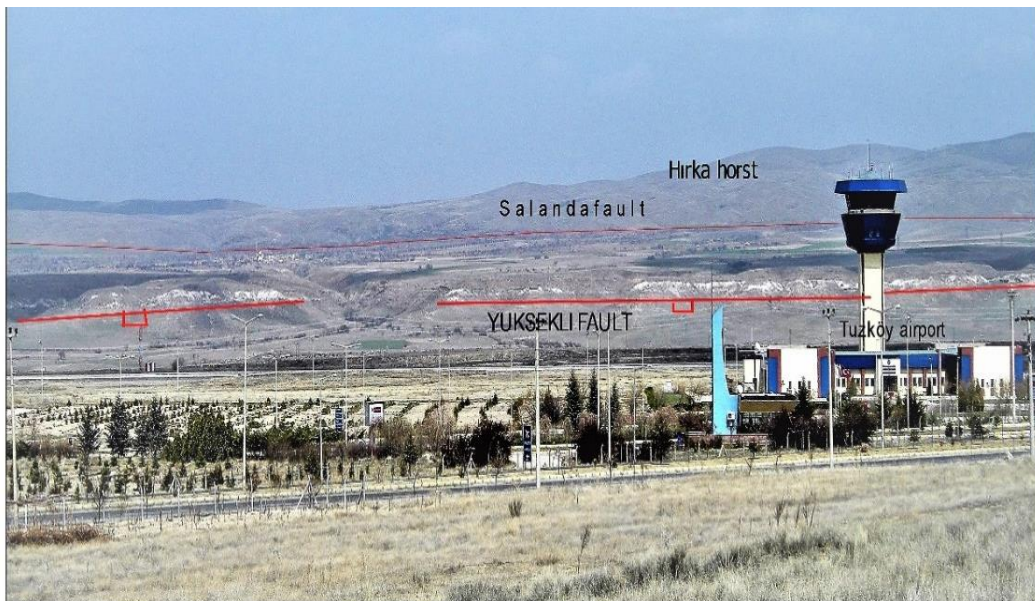


**Figure 7.** A view from the Yüksekli Fault (South of Yüksekli village).



**Figure 8.** General view of the Gülşehir fault (north of Gülşehir).

One of the faults seen in the Kızılırmak Valley is the Gülşehir fault. A typical fault delineates the valley's southern boundary. They can be viewed facing N60 to N700W. The fault planes have a northeastern dip, and their dip angles range from 56 to 620.

Additionally, the Pleistocene-aged Güvercinlik conglomerates were suspended by the Gülşehir fault. The Kızılırmak is currently resting on its current bed due to this problem. That is to say, the southern side of the Kızılırmak Valley, is the youngest fault. The Yüksekli fault is the youngest fault on the north side.

Gülşehir and its surroundings are the best places to see. It is located in the western part of the valley (Figure 8).

The research area's basement units have risen and taken on the shape of a horst structure due to faulting that is believed to be the result of the regional extensional

regime. The horst structure was developed by basement units under the influence of the extensional tectonic regime in the latter Miocene and later periods, particularly with the Salanda, Yüksekli, and Dadağı faults. The Yüksekli and Gülşehir faults emerged in the direction roughly parallel to the Salanda and Dadağı faults as a result of the extension continuing (Figure 9).

The Sarılar fault, a normal fault that strikes around N800W and dips to the southwest, is located in the northernmost portion of the research region (Figure 4).

The Yüksekli and Salanda fault planes and faults have a southwest slope direction. The Dadağı and Gülşehir faults have fault planes that are inclined northeast. This suggests that under the same tectonic regime, synthetic and antithetic faults evolved.

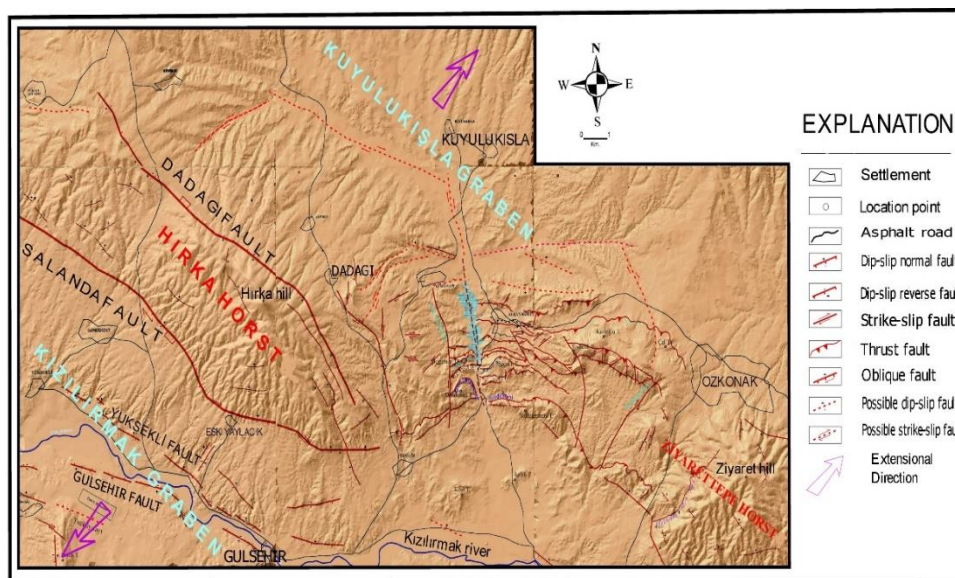


**Figure 9.** General view of the faults in the study area (Modified from Demircioğlu, 2014).

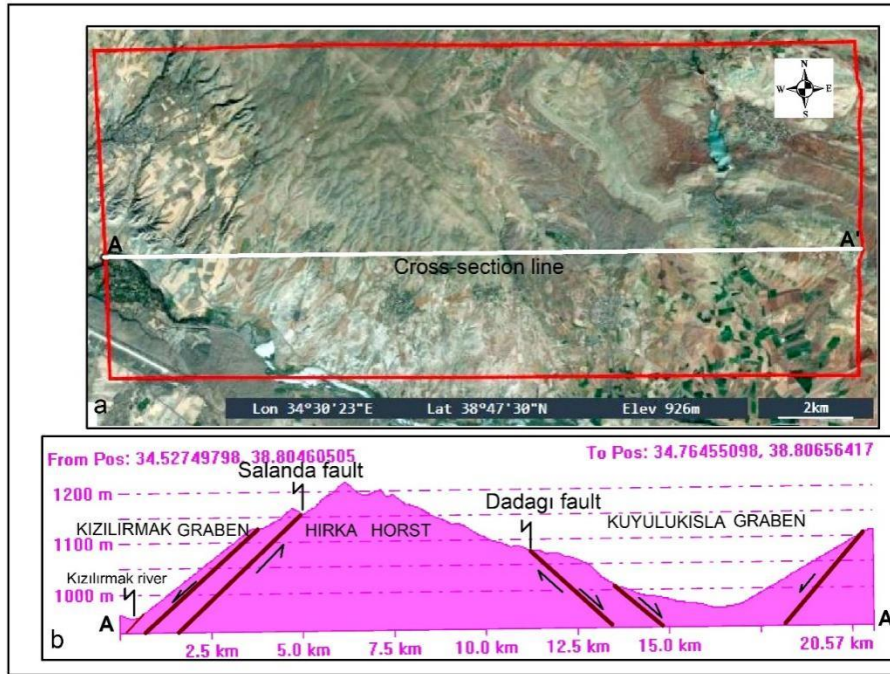


**Figure 10.** (a) Lidar image of the study area (from the Equator website, 2023), (b) Cross section obtained from the Lidar image.

Due to the extensional regime, the plain areas that remained between the normal faults produced the Kızılırmak graben, named after the Kızılırmak River, and the Kuyulukisla graben, named after Kuyulukisla Village (Demircioğlu, 2014).

Horst-graben structures were created during the Neotectonic period as a result of tension forces orientated northeast-southwest, according to the strikes of the normal faults. Due to the influence of these faults, the Kızılırmak, which originated in this region, altered its bed and eventually settled in its current location (Figure 10). A lidar image of the study area has been acquired and the faults are shown in the cross sections of this image (Figure 10).

These flaws have caused the Kızılırmak River's river bed to shift over time. Pebbles created from the sediments of the Kızılırmak River can be seen along the route between Avanos and Gülşehir.

### 3.2. Results of PSInSAR Analysis

First, the program Sentinel Application Platform (SNAP) was used to obtain interferograms. Next, data from the Shuttle Radar Topography Mission (SRTM) were utilised to eliminate the effect of topography on the interferograms. Lastly, movements in the LOS direction were obtained by using these interferograms to calculate PS points using StaMPS software. The SAR photos were analysed to ascertain the LOS direction movements occurring in the Salanda Fault. In the PSInSAR analysis, the master image was selected to be the temporal and spatial centre of all images (Figure 11).

After the SAR photos were analysed, the image was identified as the master image. A total of 333452 PS points were generated for the research region. Figure 11 displays the annual velocities in the LOS direction of the

research area along with their standard deviations. In Figure 11, the horizontal axis displays the longitude value and the vertical axis the latitude value. In Figure 11, blue colours indicate uplift and red colours indicate subsidence.

Horst-graben regions were identified using PSInSAR data (Figure 11). Horst-graben regions were identified using PSInSAR data (Figure 11). These results indicate that elevation levels are found in the horst portions and decreasing values in the graben parts. Additionally, these values agree with field findings (Figure 12).

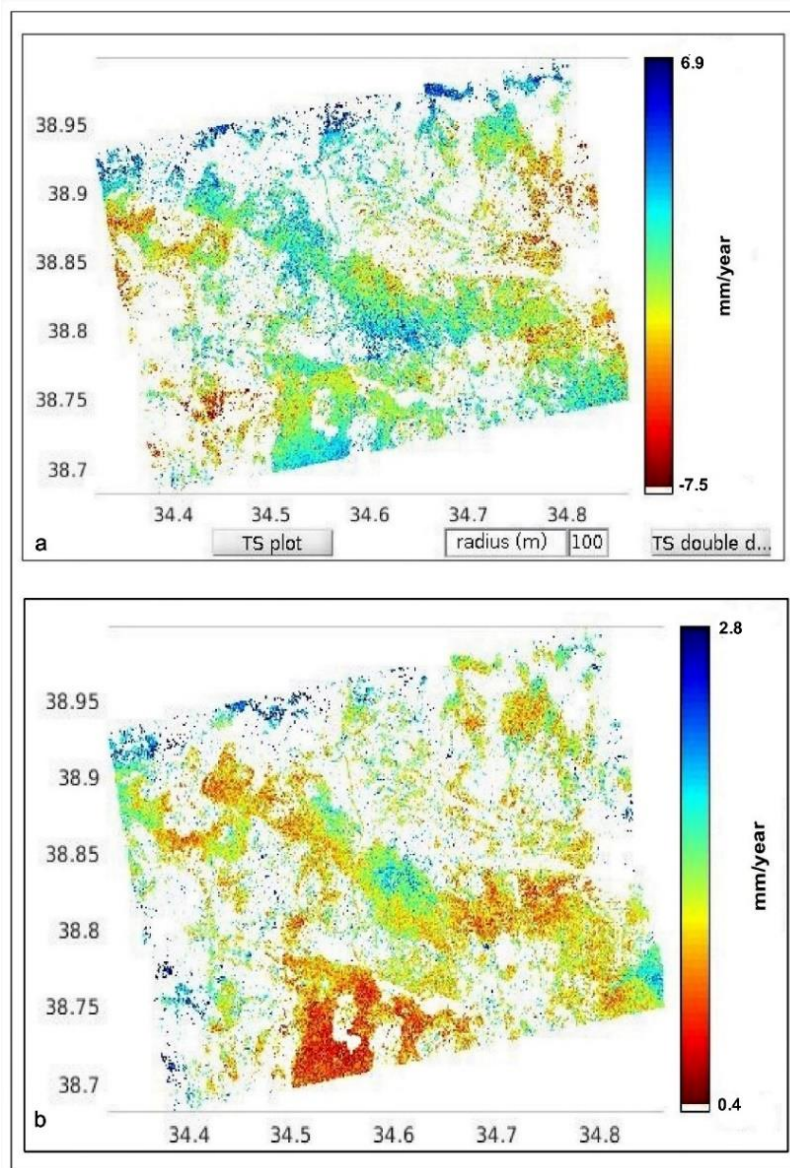


**Figure 11.** (a) PSInSAR results of the study area. Annual velocity in the LOS direction, (b) Standard deviations of the annual velocities in the LOS direction.

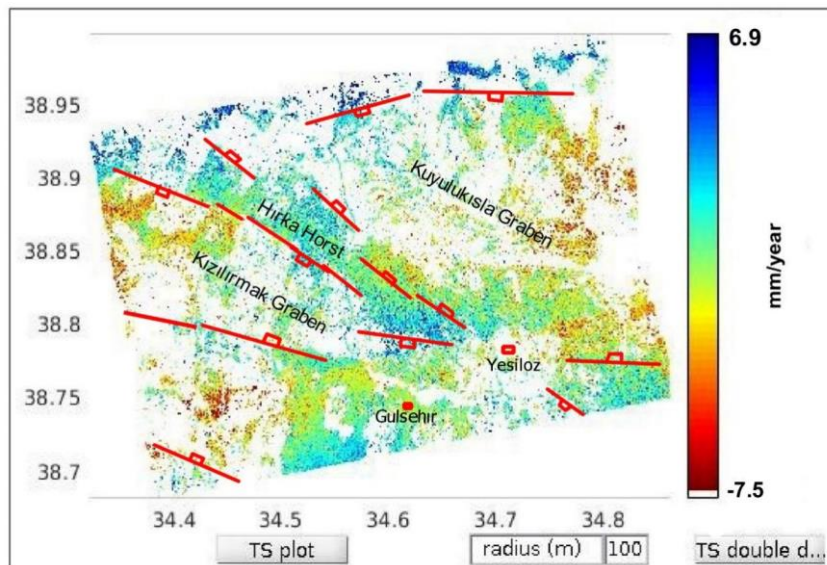


**Figure 12.** Horst-graben structures and PSInSar.



#### 4. Discussion

After the research region's annual velocities in the LOS direction were assessed, the PSInSAR analysis's findings revealed that annual uplift values of up to 7.1 mm and annual subsidence values of up to -7.5 mm had been discovered. According to Demircioğlu and Oktar (2024), these values were determined at very similar values on different measurement dates. Doğan et al. (2009) estimated that throughout the past two million years, the river digging rate along the Kızılırmak valley has been 0.08 mm/year based on field data. It was discovered that the maximum rate of excavation was 0.11 mm/year. The SAR images from this study's final three years showed an average uplift value of 6.9 mm/year.

This study is a significant improvement over the data obtained from previous studies. The evaluations made at the locations of the faults forming the Kızılırmak and Kuyulukışla grabens indicate significant uplift and subsidence values for the faults. The faults contain both horizontal and vertical movement elements. As the amount of horizontal slip is significantly reduced, the fault will not be recognised as oblique. Scholz et al. (1986) found that there are higher movement values compared to intracontinental faulting. Their study looked at the amount of movement and the tendency to cause earthquakes. As a result, these faults are likely to generate earthquakes.

#### 5. Conclusion

In this study, the PSInSAR approach was used to determine the vertical and line-of-sight motions on the faults forming the Kızılırmak and Kuyulukışla grabens. In addition, PSInSAR data were used to evaluate the actual number and amount of movements on the faults forming the grabens and horsts. The 33452 PS points generated over the study area were used to generate precise movement information about the area. The amount of movement in these places is very high due to field observations, elevations in the fault zone, and areas where the fault crosses. In terms of tectonic activity, geomorphic indices (Demircioğlu and Coşkuner, 2022) indicate moderate to high activity. PSInSAR data, field observations, and geomorphic index analyses indicate significant active faults.

#### Author Contributions

The percentage of the author(s) contributions is presented below. All authors reviewed and approved the final version of the manuscript.

	R.D.	O.O.
C	50	50
D	50	50
S	50	50
DCP	50	50
DAI	50	50
L	50	50
W	50	50
CR	50	50
SR	50	50
PM	50	50
FA	50	50

C=Concept, D= design, S= supervision, DCP= data collection and/or processing, DAI= data analysis and/or interpretation, L= literature search, W= writing, CR= critical review, SR= submission and revision, PM= project management, FA= funding acquisition.

#### Conflict of Interest

The authors declared that there is no conflict of interest.

#### Ethical Consideration

Ethics committee approval was not required for this study because of there was no study on animals or humans.

#### References

- Atabey E, Tarhan N, Yusufoglu H, Canpolat M. 1988. Hacibektaş, Gülşehir, Kalaba (Nevşehir) Himmetdede (Kayseri) arasının jeolojisi, MTA Rapor No: 8523, Ankara, Türkiye.
- Atabey E. 1989. Aksaray-H19 quadrangle, 1:100,000 scale geological map and explanatory text. Maden Tetkik Arama Yayınları Ankara, Türkiye, ss: 64.
- Aydın N. 1984. Orta Anadolu masifinin Gümüşkent B.(Nevşehir) Dolayında jeolojik petrografik incelemeler. MTA Jeoloji Etüdüleri Daire Bşk. Saydamer – Gün Kitaplığı Arşiv No: 206, Ankara, Türkiye, ss: 72.
- Biggs J, Wright T, Lu Z, Parsons B. 2007. Multi-interferogram method for measuring interseismic deformation: Denali Fault, Alaska. *Geophysical J Int*, 170(3): 1165-1179. <https://doi.org/10.1111/j.1365-246X.2007.03415.x>
- Çiner A, Doğan U, Yıldırım C, Akçar N, Ivy-Ochs S, Alfimov V, Schlüchter C. 2015. Quaternary uplift rates of the Central Anatolian Plateau, Turkey: insights from cosmogenic isochron-burial nuclide dating of the Kızılırmak River terraces. *Quaternary Sci Rev*, 107: 81-97.
- Demircioğlu R, Coşkuner B. 2022. Salanda fay zonu'nun Kesikköprü (Kırşehir) ve Yeşilöz (Nevşehir) arasında kalan kesiminin göreceli tektonik aktivitesinin jeomorfik indislerle incelenmesi. *Pamukkale Üniv Müh Bil Derg*, 8(3): 464-482.
- Demircioğlu R, Oktar O. 2024. Investigation of Salanda fault zone, between Yesiloz and Gumuskent (Nevşehir-Turkey) with PSInSAR. *Geofisica Int*, 63(2): 865-879. <https://doi.org/10.22201/igeof.2954436xe.2024.63.2.1733>
- Demircioğlu R. 2014. Geology and structural features of the Kırşehir massif and cover units in the Gülşehir-Özkonak (Nevşehir) region. PhD Thesis, Selçuk University, Institute of

- Science, Konya, Türkiye, pp: 241.
- Dirik K, Göncüoğlu MC. 1996. Neotectonic characteristics of the Central Anatolia. *Int Geol Rev*, 38: 807-817.
- Doğan U, Koçyiğit A, Wijbrans J. 2009. Evolutionary history of the Kızılırmak River, Cappadocia Section: implication for the initiation of Neotectonic regime in Central Anatolia, Turkey. 62nd Geological Congress of Turkey, April 13-17, Ankara, Türkiye, pp: e2020JD034411. <https://doi.org/10.1029/2020JD034411>
- Doğan U. 2011. Climate-controlled river terrace formation in the Kızılırmak Valley, Cappadocia section, Turkey: inferred from Ar-Ar dating of Quaternary basalts and terraces stratigraphy. *Geomorphol J*, 126: 66-81. <https://doi.org/10.1016/j.geomorph.2010.10.028>
- Eski S, Sözbilir H. 2024. Gediz (Alaşehir) grabeni'nde gelişen a-sismik yüzey deformasyonlarının kökeni. *Türkiye Jeol Bült*, 67(4): 31-62. <https://doi.org/10.25288/tjb.1342834>
- Göncüoğlu MC, Yalınz K, Kuşçu I, Köksal S, Dirik K. 1993. Orta Anadolu masifinin orta bölümünün jeolojisi, Bolum 3: Orta Kızılırmak Tersiyer Baseninin Jeolojik evrimi. T.P.A.O. Rapor No: 3313, Ankara, Türkiye, ss: 48.
- Gürsoy Ö, Kaya Ş, Çakır Z, Tatar O, Canbaz O. 2017. Determining lateral offsets of rocks along the eastern part of the North Anatolian Fault Zone (Turkey) using the spectral classification of satellite images and field measurements. *Natural Hazards Risk*, 8: 1276-1288. <https://doi.org/10.1080/19475705.2017.1318794>
- He P, Wen Y, Xu C, Chen Y. 2018. High-quality three-dimensional displacement fields from new-generation SAR imagery: application to the 2017 Ezgeleh, Iran, earthquake. *J Geodesy*, 93: 573-591. <https://doi.org/10.1007/s00190-018-1183-6>
- Hooper A, Bekaert D, Hussain E, Spaans K. 2018. Stamps/Manual, VeStamps4.1b, School of Environment, University of Leeds, Leeds, UK, pp: 135.
- Hooper A, Pa S, Howard Z. 2007. Persistent scatterer interferometric synthetic aperture radar for crustal deformation analysis, with application to Volcán Alcedo, Galápagos. *J Geophysical Res: Solid Earth*, 112: B07407. <https://doi.org/10.1029/2006JB004763>
- Koçak İ, Temiz U, Öksüz N. 2021. Salanda Fay zonu (SFZ) ile ilişkili traverten oluşumlarının paleoklimsel önemi. *Müh Bil Araş Derg*, 3: 218-225. <https://doi.org/10.46387/bjesr.963704>
- Koçyiğit A, Doğan U. 2016. Strike-slip neotectonic regime and related structures in the Cappadocia region: a case study in the Salanda basin, Central Anatolia, Turkey. *Turkish J Earth Sci*, 25(5): 393-417. <https://doi.org/10.3906/yer-1512-9>
- Koçyiğit A. 2003. Orta Anadolu'nun genel neotektonik özellikleri ve depremselliği. *Türkiye Petrol Jeologları Dern Bült*, 5(Özel Sayı): 1-26.
- Poyraz F, Hastaoglu K. 2020. Monitoring of tectonic movements of the Gediz Graben by the PSInSAR method and validation with GNSS results. *Arabian J Geosci*, 13: 844. <https://doi.org/10.1007/s12517-020-05834-5>
- Rosu AM, Pierrot-Deseilligny M, Delorme A, Binet R, Klinger Y. 2015. Measurement of ground displacement from optical satellite image correlation using the free open-source software MicMac. *ISPRS J Photogrammetry Remote Sens*, 100: 48-59. <https://doi.org/10.1016/j.isprsjprs.2014.03.002>
- Scholz C.H, Aviles CA, Wesnousky SG. 1986. Scaling differences between large interplate and intraplate earthquakes. *Bull Seism Soc Amer*, 76: 65-70. <https://doi.org/10.1785/BSSA0760010065>
- Scott C, Bunds M, Shirzaei M, Toke N. 2020. Creep along the Central San Andreas Fault from surface fractures, topographic differencing, and InSAR. *J Geophys Res: Solid Earth*, 125: e2020JB019762. <https://doi.org/10.1029/2020JB019762>
- Shirzaei M, Bürgmann R. 2013. Time-dependent model of creep on the Hayward fault from joint inversion of 18 years of InSAR and surface creep data. *Türkiye Petrol Jeologları Dern Bült*, 5(Özel Sayı): 1-25.
- Temiz U, Gökten Y.E. 2016. 10 Ocak 2016 Hacıduraklı-Çiçekdağı (Kırşehir) depremi (Mw = 5.0); ilgili yapılar ve tektonik ortam, Orta Anadolu. *Geological Bull Turkey*, 59: 155-166. <https://doi.org/10.25288/tjb.298218>
- URL-1: <https://equatorstudios.com> (accessed date: january 14, 2024).
- Wang T, Jónsson S. 2015. Improved SAR amplitude image offset measurements for deriving three-dimensional coseismic displacements. *IEEE J Selected Topics Appl Earth Observat Remote Sens*, 8(7): 3271-3278. <https://doi.org/10.1109/JSTARS.2014.2387865>
- Wang Z, Lawrence J, Ghail R, Mason P, Carpenter A, Agar S, Morgan T. 2022. Characterizing micro-displacements on active faults in the Gobi Desert with time-series InSAR. *Appl Sci*, 12(9): 4222. <https://doi.org/10.3390/app12094222>
- Yavaşoğlu H, Tarı E, Tüysüz O, Çakır Z, Ergintav S. 2011. Determining and modelling tectonic movements along the central part of the North Anatolian Fault (Turkey) using geodetic measurements. *J Geodynamics*, 51(5): 339-343. <https://doi.org/10.1016/j.jog.2010.07.003>
- Zhang X, Feng M, Zhang H, Wang C, Tang Y, Xu J, Wang C. 2021. Detecting rock glacier displacement in the central himalayas using multi-temporal InSAR. *Remote Sens*, 13(23): 4738. <https://doi.org/10.3390/rs13234738>
- Zheng M, Fukuyama K, Sanga-Ngoie K. 2013. Application of InSAR and GIS techniques to ground subsidence assessment in the Nobi Plain, Central Japan. *Sensors*, 14(1): 492-509. <https://doi.org/10.3390/s140100492>
- Zhou L, Zhao Y, Zhu Z, Ren C, Yang F, Huang L, Li X. 2022. Spatial and temporal evolution of surface subsidence in Tianjin from 2015 to 2020 based on SBAS-InSAR technology. *J Geodesy Geoinfo Sci*, 5(1): 60-72. <http://jggs.chinasmp.com/EN/Y2022/V5/I1/60>